PROCESS DESIGN AND CONTROL

Mixer-Settler Based on Phase Inversion: Design of the Mixing Zone

Joaõ B. A. Paulo[†] and Dimiter E. Hadjiev*[,‡]

Universidad Federal do Rio Grande do Norte, University Campus, Natal - RN, Brasil 59072-970, and Laboratoire de Biotechnologie et Chimie Marine, Université de Bretagne Sud, Centre de Recherche, rue Saint Maudé, 56100 Lorient, France

The aim of this work is to improve the separation efficiency in the case of liquid−liquid dispersions using a new type of mixer-settler design called MSPI (mixer-settler based on phase inversion) and a so-called solvent assisted method. The phase inversion is used to decrease the distance between the drops of the disperse phase and the interface in spherical decanters called carrier drops, while a solvent injection in the mixer allows for optimal drop diameters and, therefore, for better and easier separation. In this study, a new design method for the mixing zone in a mixer-settler is proposed. It is based on the capacity of the settler to provide high separation efficiency while throughput increases. This separation is of essential importance when residual water of good quality has to be released. A number of correlations are identified that allow reasonable prediction of the $D_{3,2}$ of carriers formed using a perforated plate, as well as the drop size distribution and the Sauter mean diameter ($\bar{d}_{min}$) of the primary dispersion. They allow predicting the influence of the organic/aqueous phase ratio as well as the contact angle on these parameters. The method is applied to design operating conditions in MSPI devices used in two particular cases, a heavy metal extraction and a crude oil emulsion separation. The results show that it is possible to obtain very good extraction efficiency coupled with good separation efficiency. They make the MSPI a viable alternative in the treatment of residual water contaminated with crude oil as well as in hydrometallurgy. At the same time the study shows that the MSPI is a simple piece of equipment to work with and very easy to maintain. While the results obtained are for some specific cases, the design methodology presented here can allow the rapid evaluation of other separation processes in the MSPI unit.

1. Introduction

It is well-known that generally, all other things being equal, the separation capacity of any sedimentation device is directly proportional to the horizontal area. Thus the most obvious effect of having extended surfaces within the sedimentation device is in the provision of additional separating area and the decrease in the rise height. This is the reason common separators using a gravity differential as the primary force include extended plate surfaces to decrease the effective rise height that must be traversed by a rising oil globule. Careful handling of flows in a gravity settler by using CPI (corrugated plate interceptor) and PPI (parallel plate interceptor) units often permits separation of oil droplets finer than those of free oil.[1] All these units are based on the lamella sedimentation principle, the theoretical background of which is Hazen's surface loading theory.[2,3]

The enhancement of the settling rate using this principle can be achieved also when applying the so-called "phase inversion method".[4−7] The phase inversion separator eliminates the main drawback of conventional settling equipment, that is, the demand for large building areas and/or volumes, while maintaining the advantages of gravity separation: simple design and low operating and overall costs.

Unfortunately gravity separation is not successful when liquid−liquid dispersions with small droplets (in the range 10−100 μm) have to be separated and especially when "stable" emulsions have to be treated. In the latter case the coalescence of the droplets is suppressed by two main mechanisms: electrostatic repulsion between charged surfaces and steric repulsion due to physical barriers. One attempt to solve these problems is the use of the so-called "solvent assisted separation method" where the droplet separation is enhanced by solvent injection in the initial dispersion. The method is a two stage continuous process where the initial dispersion and the solvent are forced into a mixing unit to form the so-called "secondary dispersion", the latter being then separated in a phase inversion separator. In this method the mixer is used to extract the initial dispersed phase into the solvent enhancing the coalescence process. At the same time a physical extraction process can decrease the part of the dissolved pollution. Appropriate conditions in the mixer allow generating "secondary emulsions" with desired mean droplet diameters, which are easily separated in the settling zone.

The main objective of this study is to propose a method for the design of the mixing section of a MSPI mixer-settler based on the optimal separation conditions in the settling zone. The goal is to improve the separation efficiency in the case of dispersions and/or emulsions while maintaining high extraction efficiency. The correlations are used to compute the separation efficiency for two industrial systems (crude petroleum in water[8] and copper extraction from acidic solutions with LIX[9]), and the predicted values are compared to the experimental ones. In this manner it is possible to show that the design methodology

* To whom correspondence should be addressed.

[†] Universidad Federal do Rio Grande do Norte, Program of Masters, Degree on Chemical Engineering.

[‡] Université de Bretagne Sud.

10.1021/ie050133z CCC: $33.50
Published on Web 04/28/2006

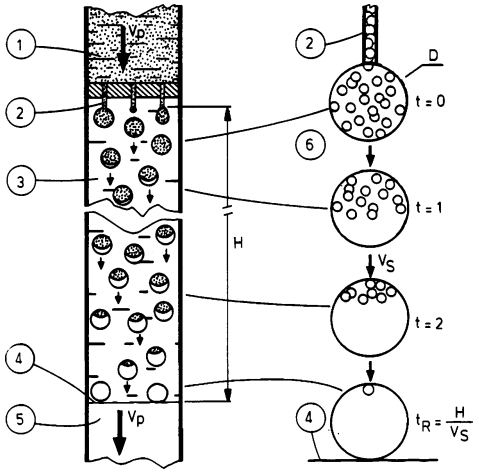

Figure 1. Phase inversion principle: 1, mixing zone; 2, nozzle; 3, organic layer; 4, organic/aqueous interface; 5, outlet aqueous phase; and 6, carrier drop.

presented here can allow the rapid evaluation of various separation processes in a mixer-settler based on phase inversion (MSPI) unit.

2. MSPI Operating Principle

The operating principle of the separator based on phase inversion has been described before.[6,8,10] It is based on the generation of "big" carrier drops containing the primary dispersion. It is important to note that each carrier works as a micro-decanter, thus decreasing the distance to the interface. A drop−drop coalescence can take place inside the carrier drop, resulting in an increase in the ascending velocity of the carried droplets and, therefore, reducing the coalescence time. The operating principle of the MSPI unit is given in Figure 1. It consists of forcing the dispersion generated in the mixer (1) through a distributor (2) with a perforated plate separating the mixer from the settling zone. The aqueous continuous phase becomes the dispersed one inside the settler. The settling zone (3) is filled with an organic phase identical to the originally dispersed one. The motion of the carriers toward the interface (4) is governed by a residence time $T_R = H_o/U_s$, where H_o is the height of the organic layer and U_s is the sedimentation velocity of the carrier drop. The carried droplets (less dense) tend to ascend inside the carriers (more dense) thus concentrating in the upper part and coalescing in the organic bed. The noncoalesced droplets can still be recovered near the interface.

3. Introduction to the Design Method

3.1. Separation in the Settling Zone. In the settling zone, the internal circulations induced in the "carrier" drops during their formation are always present. It can be assumed that during the sedimentation of the carriers the velocity of these internal circulations decreases and some coalescence between the "carried" microdroplets might occur. On the other hand the coalescence on the oil−"carrier" drop interface is hindered by the presence of this internal movement. Thus the height of the organic band may influence considerably the separation process. At the same time, big carriers assume flattened, ellipsoidal shapes and fall in a zigzag or spiral pattern. This motion increases dissipation and drag, and the settling rate may actually decrease with increasing carrier diameter but does not enhance separation because of the interface phenomena mentioned below.

Recently[10] the dimensional analysis was used to assist in the interpretation of these complex phenomena. It was assumed that the separation efficiency is governed by the physicochemical properties of the system, the droplet Sauter mean diameter, and the continuous phase flow rate, in that order, as well as the throughput and some geometrical characteristic of the device. So

$$E = f(\rho_0, \rho_{aq}, \mu_0, \mu_{aq}, \sigma, g, d, d_N, H_o, U_N) \qquad (1)$$

Some of these variables, namely, the nozzle diameter d_N, the velocity U_N, and the physicochemical properties of the system, govern the carrier drop formation. The relation between the viscosity force, the surface tension force, and the inertial force was introduced using the Ohnesorge number Z:

$$Z = \frac{\mu_{aq}^{\ 2}}{d_N \rho_{aq} \sigma}$$

During its movement through the organic band a drop can deform and the deformation is opposed by the surface tension. According to the observed phenomena not only can the interface deform, but it also moves along with the surrounding liquid. This interfacial mobility appears to be opposed by two phenomena: dissipation in the drop and occurrence of surface tension gradients tending to immobilize the interface. To take into account the effects during the motion in the organic band the Morton number *Mo* was introduced:

$$Mo = \frac{g \Delta\rho \mu_{aq}^{\ 4}}{\rho_{aq}^{\ 2} \sigma^3}$$

Dimensionless groups such as d/d_N, $d/D_{3,2}$, and $D_{3,2}/H_o$ were used to characterize the operating conditions, and the effect of the drop and organic phase viscosity is also taken in account (μ/μ_{aq}).

The final form of the equation has been proposed as follows:[10]

$$E = 586.73 + 19.245 \ln\left[\left(\frac{d}{d_N}\right)\left(\frac{D_{3,2}}{H_o}\right)^{0.4}\left(\frac{d}{D_{3,2}}\right)^{2.2} Z(Mo)^{0.149}\left(\frac{\mu_o}{\mu_{aq}}\right)^{0.14}\right] \qquad (2)$$

Many experimental results have confirmed that in all cases when the parameter $X = (d/d_N)(D_{3,2}/H_o)^{0.4}(d/D_{3,2})^{2.2} Z Mo^{0.149} (\mu_o/\mu_{aq})^{0.14}$ exceeds 1×10^{-11} the separation is practically total. Below this value the separation efficiency can be computed using eq 2. In this case, the average deviation between the proposed equation and the experimental data is about ±7%.

Therefore, for a given system and an existing device it can be easily shown that the condition for complete separation can be written as

$$X = A\left(\frac{d^{3.2}}{(D_{3,2})^{1.8}}\right) = 1 \times 10^{-11} \qquad (3)$$

with

$$A = \left[\left(\frac{1}{d_N H_o^{\ 0.4}}\right) Z(Mo)^{0.149}\left(\frac{\mu_o}{\mu_{aq}}\right)^{0.14}\right]$$

Thus, if $D_{3,2}$ is known, one can determine the minimal mean diameter ($\bar{d}_{min}$) to be completely separated in a given device. The Sauter mean diameter of the carrier ($D_{3,2}$) is, therefore, of essential importance to the design of the MSPI unit.

3.2. Carrier Drop Formation. The mixer and the settling zone are separated by a perforated plate (3), where "carrier" drops are formed. This one is characterized by high velocities in the nozzles. In most cases the drop formation occurs in the jet regime,[11,12] and internal circulations are induced in the carriers. Thus, the phenomena here may influence both the drop size D, the internal circulation velocity, and correspondingly the separation process. Experiments with various types of perforated plates have clearly outlined that reproducible phenomena are most readily obtained with plates of nonwetting materials so that the dispersed phase (the aqueous phase) could not spread over or wet the outer surface. At the same time the nozzle length l_N has to be several times greater than its diameter. As it was mentioned before, the nozzle diameter d_N, the velocity U_N, and the physicochemical properties of the system are governing the carrier drop formation. According to these parameters and the plate wettability, there are two modes to generate liquid droplets in a stagnant liquid while another liquid is flowing through an orifice: in intermediate regime conditions and in jet regime conditions. Skelland and Johnson[13] have determined the critical jet diameter and the minimal critical velocity in the nozzle, U_c. If the nozzle velocities remain always lower than the critical one, according to correlations given by Dalingaros et al.[14] the diameter of drops formed in a scattering plate can be calculated using the Weber (We) and the Eötvos ($Eö$) dimensionless groups as follows:

$$\frac{D_{3,2}}{d_N} = \frac{4}{3}\left[\frac{6 - 2We}{Eö}\right]^{0.25} \quad \text{when} \quad 0 < We < 2$$

$$\frac{D_{3,2}}{d_N} = 2.35(We)^{-0.55}Eö^{-0.16}\exp(0.08We) \quad \text{when} \quad 2 < We < 8.64$$

with

$$We = \frac{\Delta\rho d_N U_N{}^2}{\sigma} \quad \text{and} \quad Eö = \frac{\Delta\rho d_N{}^2 g}{\sigma}$$

The use of the nozzle diameter (d_N) in the Eötvos dimensionless group can be attributed to the assumption that the radius of the drop (R) is equal to x times the nozzle diameter at time t, where x is the correction factor to account for the dependency of drop size on the nozzle diameter (similar to the static drop size dependency on a capillary diameter).

Previous studies,[9] with plates of hydrophobic materials, have shown, however, that these correlations, proposed for a single phase flow, cannot be used when a biphasic system flows through a perforated plate. Zhang[15] has studied the effect of inertial, gravitational, and surface tension forces on the dynamics of liquid drop formation from a nozzle. He considered the case of a drop of an incompressible Newtonian liquid forming into a quiescent, dynamically inactive ambient fluid, with the drop liquid injected at a constant flow rate. It was found that the major parameters governing the dynamics of drop formation are represented by the Reynolds number $Re = U_N d_N \rho/\mu$, the capillary number $Ca = U_N\mu/\sigma$, the gravitational Bond number $Bo = R_N{}^2 g\rho/\sigma$, and the ratio of inner R_i and outer radii of the nozzle (here the contact radius R_c is the radius of the surface wetted by the liquid). This ratio has been found experimentally to have little effect on the drop volume but affects the flow pattern significantly in the period of drop growth. The value of R_i/R_c influences the thread breakup and generation of satellite droplets. As the contact radius depends on the contact angle, and, therefore, on the wettability of the solid surface, the liquid dispersion has to be realized using plates of hydrophobic materials ("nonwetted" by the dispersed aqueous phase). Further, it was confirmed that the maximum limiting length that a drop attains prior to its breakup and the volume of a drop that breaks off from a nozzle increases significantly with increasing Reynolds and capillary numbers and with decreasing gravitational Bond number (which is twice the $Eö$). Obviously, the dynamic of drop formation is a strong function of the relative importance of the inertial to surface tension forces and a weak function of the gravitational force.

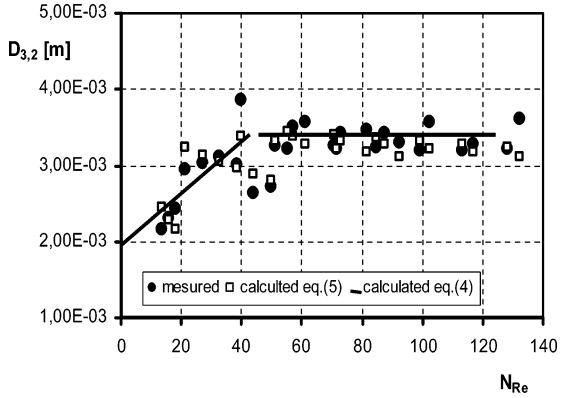

Figure 2. Influence of Re on the Sauter mean carrier drop diameter ($D_{3,2}$) (Solvesso 150−water; U_N = 0.118−0.274 m·s^{-1}; Q = 16.8−39.1 m^3·m^{-2}·h^{-1}). Comparison between experimental and calculated values.

The drop formation depends on the hydrodynamic conditions and, therefore, on the Reynolds dimensionless group (Re) as it can be seen in Figure 2, where results obtained in ref 9, where the diameter of the carrier drops has been measured experimentally, are presented. For the determination of Re in biphasic systems, volume averaged density values were used, while viscosity values were calculated using[16]

$$\mu_m = \frac{\mu_{aq}}{1-\phi}\left(1 + \frac{1.5\phi\mu_{org}}{\mu_{aq} + \mu_{org}}\right)$$

where ϕ is the volume fraction of the dispersed phase and μ_{aq} and μ_{org} are the viscosities of the aqueous and the organic phases, respectively. As expected, the volume of the drop increases monotonically as the Reynolds number increases from 0.1 to about 50, due primarily to the increase in the inertial force. At this critical Re ($Re \approx 50$), transition to jetting occurs, at which time the volume of the drop attains its maximum.

When the viscosity values calculated above are used, the capillary dimensionless number Ca has also been computed. The effect of this parameter on drop breakup in terms of detaching the volume of the drop has been estimated. The volume of the drop increases considerably with increased capillary number. Therefore, higher organic phase contents lead to smaller carriers as it can be seen in Table 1. Finally two correlations are proposed here to estimate the Sauter mean diameter of a carrier drop:

$$D_{3,2} = 3\times10^{-9}Re^3 - 7\times10^{-7}Re^2 + 6\times10^{-5}Re + 0.0017 \quad \text{for} \quad Re \le 50 \quad (4)$$

for $Re \ge 50$ one assume $Re = 50$.

For a given system the capillary number is proportional to the Reynolds number. So, if the capillary number is used, then

$$D_{3,2} = 0.0036e^{-10.36Ca} \quad (5)$$

Table 1. Comparison between Experimental and Calculated Diameters (Nozzle Diameter 0.7 mm)

			$D_{3,2}$ (measured) [mm]				$D_{3,2}$ (eq 5) [mm]			
Q [m³·m⁻²·h⁻¹]	U_N [m·s⁻¹]	$D_{3,2}$ (ref 14) [mm]	$\phi = 0.1$	$\phi = 0.25$	$\phi = 0.5$	$\phi = 0.75$	$\phi = 0.1$	$\phi = 0.25$	$\phi = 0.5$	$\phi = 0.75$
16.8	0.118	3.58	3.21	3.87	2.94		3.44	3.38	3.23	
21.6	0.151	3.53	3.26	3.26	3.03		3.40	3.32	3.13	
25.8	0.181	3.48	3.23	3.57	3.12	2.17	3.35	3.27	3.05	2.49
30.2	0.212	3.41	3.19	3.22	3.02	2.30	3.31	3.22	2.96	2.29
34.6	0.242	3.32	3.19	3.46	2.64	2.44	3.28	3.17	2.88	2.15
39.1	0.274	3.18	3.21	3.31	2.71		3.23	3.12	2.79	

A comparison between experimental and calculated (eqs 4 and 5) mean carrier diameters is given in Table 1 and in Figure 2. As it can be seen in Figure 2, the correlation based values tend to match the experimental ones with good precision. The average deviation between the proposed eq 5 and the experimental data is about ±10%, while that for the proposed eq 4 is about ± 20%.

3.3. Design of the Mixing Zone. Once the $D_{3,2}$ value is determined, one can easily calculate the minimal solvent drop diameter ($\bar{d}_{min}$) of the carried droplets that might be completely separated in a given device. The next step is to determine the corresponding hydrodynamic conditions in the mixer allowing for drop sizes equal or higher than $\bar{d}_{min}$. So $\bar{d}_{min}$ becomes the minimal solvent drop diameter to be generated in the mixer if high separation efficiency has to be obtained.

In extraction−separation the drop size distribution in the mixer will be primarily determined by the competing phenomena of drop breakup and coalescence. From the different suggested mechanisms, breakup in the inertial subrange of turbulence will be the prevailing one in dilute dispersions.[17] The maximum drop size that can resist breakup, d_{max}, will depend on the balance between the stresses generated by external turbulent fluctuations, which tend to break the drops, and the surface tension, which tends to stabilize them. In stirred vessels d_{max} will be given by

$$d_{max}/d_{imp} \propto (We_{imp})^{-0.6}$$

where $We_{imp} = \rho_{aq}N^2d_{imp}^3/\sigma$ is the stirred tank Weber number.[16] The maximum droplet size is thus determined by the continuous phase density ρ_{aq}, the impeller rotational speed N, the impeller diameter d_{imp}, and the interfacial tension σ. The dispersed phase viscosity can help to stabilize the drops, and its effect is often accounted for by introducing a viscosity number. This can, however, be ignored for systems with small viscosity differences between phases.

Coalescence of drops will occur at high dispersed phase volume fractions and will result in increased drop sizes. The mechanisms relevant to drop−drop coalescence have been detailed by Chester.[18] However, even when coalescence is prevented, increasing the volume fraction of the dispersed phase will decrease the turbulence intensity and, therefore, increase the dispersed phase droplet size.

Instead of d_{max}, a more useful parameter, particularly in our case as well as for mass transfer operations, is the Sauter mean diameter in the mixer (in our case $\bar{d}$ instead of $d_{3,2}$), which is assumed to be proportional to d_{max}. The effect of the phase fraction upon the resulting mean diameter has been thoroughly studied, and the results are often presented as a linear concentration correction function or a power function with the general form

$$\frac{\bar{d}}{D_{imp}} = c_1(1 + c_2\phi)^n(We_{imp})^{-0.6} \qquad (6)$$

Therefore, it can be said that for a constant impeller speed, an increase in the volume fraction of the dispersed phase results in larger drops in the mixer. This correlation has been found to be dependent on the coalescence rates. A number of correlations taking the form of eq 6 have been proposed in the literature, the most relevant being given in ref 16. In the case of low coalescence rate systems, the mean diameter can be considered as a linear or quasi linear function of the volume phase fraction.[19] In this case the constant c_2 can be considered equal to 3 when it accounts for turbulence damping at low dispersed phase concentrations,[20] while it is higher than 3 for coalescing systems.[21] At high dispersed phase volume fractions (above 0.4), however, a further increase in the dispersed phase concentration results in decreasing drop size.[17,22] This behavior can be attributed to alternative mechanisms of drop breakup such as capillary breakage produced by the elongational flow inside the impeller blades. This modification of the breakage mechanisms at high phase ratio has been recently confirmed by drop size measurements with a laser granulometer.[23] The typical drop size volume distribution is a bimodal distribution composed of a primary distribution centered around the mean diameter and a residual one centered around a smaller diameter. The ratio of the mean diameter of this primary dispersion to the mean diameter of the residual one is found to be unaffected by the phase ratio, and the order of magnitude is in good agreement with Stone's numerical predictions.[24] The most important conclusion, with respect to the design of MSPI units, is that it is possible to use eq 6 to calculate the mean diameter in various systems with different proportionality constants depending on the breakup mechanisms on the liquid−liquid interface. The effect of the volume fraction on the mean diameter is given by a linear relationship with higher slope for the coalescing systems than that for the noncoalescing ones.

Thus, using the already proposed eq 6, it is possible to determine the impeller rotation speed in the mixer allowing for drop sizes equal to or higher than $\bar{d}_{min}$ and, therefore, the conditions for optimal separation in a MSPI unit of a given geometry. It should be added that, in the solvent assisted method, the mixer is used as a dynamic coalescer rather than as a mixing device. So parameters concerning the coalescence process have to be added allowing for a correct design of the mixing zone.

4. Experimental Section

4.1. Reactor Geometry and Operating Conditions. Data obtained with two MSPI units and two systems are used to show the possibility of designing the operating conditions in the mixing zone using the new method. The scheme of a MSPI unit is given in Figure 3, and the main geometrical characteristics of the units are given in Table 2. Both phases are forced through the mixer by means of centrifugal pumps (1, 2). The mixing chamber (4) is a glass tube containing four baffles. The mixer impeller (5) is a four-blade turbine 44 mm in diameter designed to minimize the formation by shear of very fine droplets. These slow settling droplets are the major cause of haze in the settler,

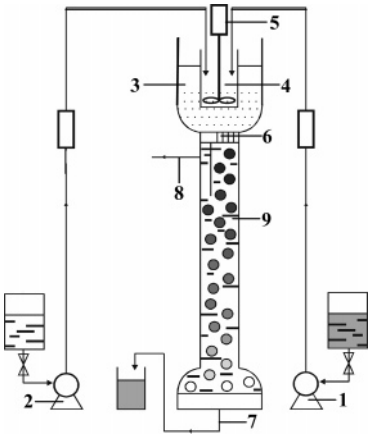

Figure 3. Experimental setup: 1 and 2, pumps; 3, mixer; 4, mixing zone; 5, driving motor with impeller; 6, scattering plate; 7 and 8, aqueous and organic phase outlets; and 9, organic layer.

giving rise to high organic losses in the outlet aqueous phase. The impeller is provided with a driving motor allowing a smooth increase in the impeller speed. The speed was maintained constant during all experiments. The continuous phase flow rate is controlled and measured. This continuous phase is an aqueous copper solution in the case of copper extraction and an oil-in-water dispersion in the case of crude petroleum−water separation. The extractant (solvent) coming from the tank is pumped into the mixer after controlling and measuring its flow rate. The mixed phases enter the upper part of the settling zone (9) and flow through the scattering plate (6). It is a perforated plate (Teflon in the case of copper extraction and Technyl−nylon 6 in the case of crude petroleum separation) with 5.1% of free surface and a hole diameter of 1 mm. The settler is an acrylic tube. This material has been chosen because of its hydrophobicity (contact angle of 149°) which limits the formation of a bed of uncoalesced drops. These beds, very useful in the case of fine dispersion separations,[6] can limit the throughput capacity.

Table 3 shows the physicochemical properties of the systems used. The contact angle has been determined on thin pieces of plastic materials using a Digidrop MSE contact angle meter and the size distribution using a Malvern 2600 granulometer. More details concerning the analysis of the feed and outlet solutions as well as the estimation of the separation efficiency can be found in refs 7, 9, and 10.

4.2. Heavy Metal Extraction in a MSPI Unit. The use of a MSPI unit as a classic mixer-settler has already been studied.[9] In this case mixing allows for good phase dispersion and suitable mass transfer coefficients. In the case of a fast chemical reaction and a large amount of extractant, the agitation speed and the throughput become the parameters governing the extraction−separation process. Therefore, it is suitable to realize a preliminary test with the new design method in these conditions.

Table 4. Comparison between Experimental and Calculated Separation Efficiency for the Case of a Heavy Metal Extraction Process

specific throughput [$m^3 \cdot m^{-2} \cdot h^{-1}$]	U_N [$m \cdot s^{-1}$]	phase ratio O/A	E calcd [%]	E exptl [%]
16.8	0.118	0.10	97.7	99.64
21.6	0.151	0.10	98.2	99.57
25.8	0.181	0.10	98.6	99.50
30.2	0.212	0.10	99.0	99.40
34.6	0.242	0.10	99.4	99.23
39.1	0.274	0.10	99.9	99.20
16.8	0.118	0.25	100.0	99.90
21.6	0.151	0.25	100.0	99.80
25.8	0.181	0.25	100.0	99.76
30.2	0.212	0.25	100.0	99.71
34.6	0.242	0.25	100.0	99.70
39.1	0.274	0.25	100.0	99.69
16.8	0.118	0.50	100.0	99.94
21.6	0.151	0.50	100.0	99.95
25.8	0.181	0.50	100.0	99.93
30.2	0.212	0.50	100.0	99.93
34.6	0.242	0.50	100.0	99.92
39.1	0.274	0.50	100.0	99.30
16.8	0.118	0.75	100.0	99.99
21.6	0.151	0.75	100.0	99.99
25.8	0.181	0.75	100.0	99.98
30.2	0.212	0.75	100.0	99.98
34.6	0.242	0.75	100.0	99.98
39.1	0.274	0.75	100.0	99.98

In ref 9, the characteristics of a MSPI unit were studied using acidic copper solutions and LIX 984 (Henkel Corp.) as extractant. The initial copper concentration in the aqueous phase was approximately 1.5 g/L, and the pH was 2−3. The organic phase was a 5.2 vol % of LIX 984 in Solvesso 150. Results, for the influence of the throughput and the phase fraction on the separation efficiency (already obtained in ref 9), are given in Table 4 and compared to those predicted by the new design method (eqs 2, 3, 5, and 6). As it can be seen, the average deviation between the proposed method and the experimental data is up to be ±2%, the most important being that at low phase fractions.

The experimental results show also that by increasing the throughput the separation efficiency very slightly decreases, while the predicted values show the opposite trend. This can be attributed to coalescence phenomena on the oil−water interface at the bottom of the unit. The coalescence of a carrier on this interface can be so vigorous that the drainage of the

Table 2. Reactor Characteristics

	mixing zone								separator	
MSPI for	d_{imp} (mm)	d_{imp}/D_m	H_m/D_m	no. of baffles	no. of blades	Y/d_{imp}	no. of impellers	b/D_m	D_s (m)	H_s (m)
extraction	44	0.37	2.92	4	6	1	1	0.1	0.05	0.5
oil separation	44	0.55	1.375	4	6	1	1	0.1	0.05	1

Table 3. Physical Properties of the Systems Used

system		organic phase			aqueous phase		eq 6	
continuous phase	solvent	μ (mPa·s)	ρ (kg/m^3)	σ (mN/m)	μ (mPa·s)	ρ (kg/m^3)	C_1	C_2
aqueous copper solution	LIX in Solvesso	1.58	779.0	38.1	1.19	979	0.056	1.36
formation water + crude oil (1)	Turpentine	1.00	760.0	27.29	0.65	1055	0.15	0.6
formation water + crude oil (2)	hydrocarbon mixture (called aguarras)	1.00	763.8	27.29	0.65	1055 (150 mg/L of colloidal clay particles)	0.056	3.6
	crude oil	1000	871.8					

organic film cannot be terminated. The use of a microscope−camera system has shown the formation below this interface of a newborn population of fine dispersed droplets. Part of them are entrained with the aqueous phase, which, therefore, influences the separation efficiency. Granulometric analyses have confirmed these observations and have been detected at the outlet droplets having diameters not present in the inlet flow.

The comparison between the experimental and the calculated efficiencies gives very good results with very little scattering. Therefore, the possibility to use the new method to design the mixing zone in a MSPI unit is confirmed. It should be added that in all cases the extraction efficiency was higher than the separation one (approximately 100%).

4.3. Dynamic Coalescence in the Mixing Zone. Emulsions are thermodynamically unstable systems which, given the opportunity, would separate through coalescence of the dispersed droplets. In a "stable" emulsion, coalescence is suppressed by two main mechanisms: electrostatic repulsion between charged surfaces in an electrolyte and steric repulsion due to physical barriers. Yeung et al.[25] have recently studied the coalescence of emulsified oil drops. They found that, when two droplets without a steric layer are brought together on direct approach, coalescence is rarely observed, while it is facilitated by a lateral shearing. In fact, in a real industrial dispersion of crude oil-in-formation water, both mechanisms are present: the oil droplets are charged negatively (charges due to the dissociation of carboxyl groups), and the emulsion contains colloidal clay particles. The solvent assisted method is an attempt to solve this problem. In fact, if an organic solvent is added to the emulsion, the coalescence between oil droplets may be replaced by coalescence between oil and solvent droplets. Thus, by choosing a suitable solvent, a practically "stable" emulsion can be transformed into an unstable system.

When a solvent is injected into the mixing zone of the MSPI unit, the latter acts as a dynamic coalescer. Therefore, parameters governing the coalescence process are of essential importance. Studies on the coalescence[26] have shown that, in the flow driven coalescence process, the coalescence rate increases with increasing particle concentration and that the coalescence efficiency decreases with increasing shear rates. This can be qualitatively explained in the first case by increased number of collisions and in the second case in terms of particle deformation and hydrodynamic interactions related to the trajectories of particles. Further, a decrease in coalescence efficiency can be observed when the particle sizes differ.[26] The method being based on the coalescence between oil droplets and solvent drops, it is evident that the coalescence rate determines the separation efficiency in the MSPI unit.

In the case of a solvent assisted separation, the agitation speed determines the size of the solvent droplets and, therefore, the number of particles for a given phase ratio. An increase in solvent injection (phase ratio O/A) results in an increase of the above-mentioned number of particles, increasing the coalescence efficiency. Thus, it can be clearly outlined that these two parameters coupled with the viscosity ratio reflect the most important operating conditions in the mixing zone according to the main mechanism of coalescence, which is the improved Smoluchowski theory (called trajectory theory).

4.3.1. Experiments with the Industrial Wastewater (Formation Water−Oil and Turpentine as Solvent). The oil separation using the MSPI unit, a turpentine as solvent, and a real industrial dispersion of crude oil-in-formation water coming from PETROBRÁS/E&P-RNCE (Ceará basin/Mandaú subbasin and from the fields of Xeréu and Atum) has been studied before, and the advantages of the solvent assisted method have been outlined.[27] Thus, it was shown that the solvent injection in the mixer allows extracting the fine droplets into the solvent drops formed during the mixing. It is, therefore, possible to control the agitation speed to control their diameters and, therefore, to improve and accelerate the separation.

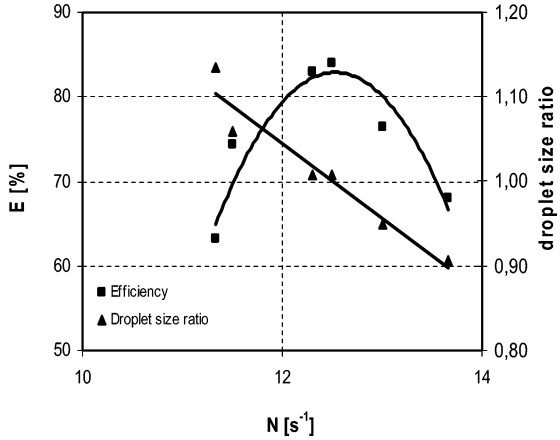

Figure 4. Influence of the impeller speed on the carried droplet size and the separation efficiency ($U_N = 0.283$ m·s^{-1}; $O/A = 0.33$; $N = 660 \div 780$ rpm; initial oil concentration 0.733−1.214 kg·m^{-3}; $Q = 40.76$ m^3·m^{-2}·h^{-1}).

A new set of experiments with the same solvent has been used to determine the optimal conditions in the mixing zone. The influence of the initial oil content in the crude oil/formation water dispersion, the specific throughput Q (m^3·m^{-2}·s^{-1}), the solvent to effluent phase ratio (O/A), and the agitation speed upon the mean separation efficiency were studied. The generated mean solvent droplet diameter ($\bar{d}$) of the solvent dispersion was estimated using the constants c_1 and c_2 given in Table 3. These constants have been obtained experimentally for various systems and organic phase contents using a Malvern 2600 laser granulometer. As it can be seen, they depend on the system and do not match the values given by other authors[16,28] in similar conditions for a large range of dispersed phase concentrations. This is probably due to the fact that the deformation and the breakup mechanisms on the liquid−liquid interface cannot be reduced to a single parameter (the interfacial tension). The partial adsorption of Cl^- ions at the interface (initial Cl^- content in the formation water of 78.75 mg Cl^-·L^{-1}) can be an acceptable explanation for the very low coalescence rate observed with this system.[28]

The influence of the agitation speed was studied without bed formation and with an organic layer height in the settler of 0.75 m. The inlet crude oil concentration was in the range from 0.733 to 1.214 kg·m^{-3}. The throughput was maintained constant and equal to 40.76 m^3·m^{-2}·h^{-1}, and $O/A = 0.33$. The mean carrier diameter $D_{3,2} = 3.21 \pm 0.1 \times 10^{-3}$ m was calculated using eq 5. The results obtained, presented in Figure 4, confirm the role of the solvent dispersion in the coalescence process. It was found that the coalescence rate (i.e., the separation efficiency) does not change monotonically with increasing the agitation speed. Instead, with increasing agitation speed, the coalescence efficiency increased first and then decreased. These results directly confirm the importance of hydrodynamic interactions between droplets due to trajectories as proposed by Zeichner and Schowalter.[29] As it can be seen in Figure 4, by increasing the agitation speed the generated mean droplet diameter ($\bar{d}$) of the solvent dispersion decreases, changing therefore the mean droplet-size ratio ($\bar{d}/\bar{d}_{oil}$). According to the trajectory theory the coalescence efficiency decreases when the droplet sizes differ. Theoretically, the higher efficiency can be obtained for colliding

Table 5. Comparison between Experimental and Calculated Separation Efficiencies for Various Operating Conditions (Solvent Turpentine)

fixed parameters		variable parameters			separation efficiency		coalescence parameters		
organic bed height (H) [m]	stirring speed [rpm]	initial oil content [kg·m^{-3}]	specific flow rate (Q) [m^3·m^{-2}·h^{-1}]	phase ratio (O/A)	exptl [%]	calcd [%]	deviation [%]	Choc probability $N_{oil}/N_{solvent}$	drop-size ratio $\bar{d}_{oil}/\bar{d}_{min}$
1	750	0.041	26.50	1/3	58.53	78.38	33.91	0.02	1.01
1	750	0.041	39.75	1/1	73.17	75.86	−3.67	0.01	1.09
1	750	0.041	46.37	1/6	76.58	79.15	−3.25	0.03	0.97
1	750	0.088	26.50	1/3	84.00	79.65	5.18	0.04	0.99
1	750	0.088	33.12	1/3	86.10	80.71	6.26	0.04	0.99
1	750	0.088	40.76	1/3	88.50	81.70	7.68	0.04	0.99
1	750	0.519	26.50	1/3	96.30	96.62	−0.33	0.25	0.99
1	750	0.519	33.12	1/3	97.00	97.90	−0.93	0.25	0.99
1	750	0.519	40.76	1/3	97.30	99.10	−1.85	0.25	0.99
1	750	0.766	26.50	1/3	96.60	96.62	−0.02	0.37	0.99
1	750	0.766	33.12	1/3	97.10	97.90	−0.83	0.37	0.99
1	750	0.766	40.76	1/3	97.30	99.10	−1.85	0.37	0.99
1	750	1.004	39.75	1/5	98.00	96.81	1.22	0.71	0.97
1	750	1.004	45.86	1/5	99.00	97.63	1.38	0.71	0.97
1	750	1.004	51.97	1/5	99.80	98.35	1.45	0.71	0.97
1	750	1.348	26.50	1/3	99.10	96.62	2.50	0.64	0.99
1	750	1.348	33.12	1/3	99.30	97.90	1.41	0.64	0.99
1	750	1.348	40.76	1/3	99.50	99.10	0.40	0.64	0.99
1	750	4.609	26.50	1/3	99.60	96.62	2.99	2.21	0.99
1	750	4.609	33.12	1/3	99.70	97.90	1.80	2.21	0.99
1	750	4.609	40.76	1/3	99.80	99.10	0.70	2.21	0.99

droplets of equal size ($\bar{d}/\bar{d}_{oil} = 1$). The experiments show this value to be equal to 1.02 ($N = 750$ rpm). It can be assumed, therefore, that the optimum mean droplet ratio is in the range of 1.0 ± 0.1. It should be noted that in the case of oil-in-water/solvent coalescence the viscosity ratio of the organic phases is very low (0.001) allowing for a high coalescence rate and for optimum separation efficiency.

The influence of the initial oil content in the crude oil/formation water dispersion and the specific throughput Q (m^3·m^{-2}·s^{-1}) upon the mean separation efficiency was also studied. The experiments were carried out without bed formation and with an organic layer height in the settler of 1 m. The inlet crude oil concentration was in the range from 0.041 to 4.609 kg·m^{-3}, the O/A ratio was 0.33, and the total flow rate ranged from 26.50 to 51.97 m^3·m^{-2}·h^{-1}. The mean carrier diameters $D_{3,2}$ were calculated using eq 5. The results obtained, presented in Table 5 and in Figure 5, confirm the fact that the higher the oil content in the inlet flow, the better the separation. For inlet concentrations of 0.088 kg·m^{-3} the separation efficiency obtained is approximately 86%, whereas for an inlet concentration of 4.609 kg·m^{-3} this efficiency is 99.7%. The lower separation efficiency for lower concentrations can be attributed to the coalescence phenomena in the mixing zone. According to Smoluchowski's theory, this can be explained by a decreased number of collisions. Results obtained with various throughputs, given in Figure 6, confirm that the lower separation efficiencies are always observed for initial oil contents up to 0.1−0.2 kg·m^{-3}. It should be also added that by increasing the throughput the separation efficiency increases slightly, which is due to a decrease in the mean carrier diameter. When the specific throughput increases from 25.50 to 46.37 m^3·m^{-2}·h^{-1} this diameter decreases from 3.67×10^{-3} to 3.49×10^{-3} m. In this manner, separators based on phase inversion can increase their separation efficiency while increasing throughput, which can be obtained neither in gravity settlers nor in coalescing devices. At the same time the low residual organic concentration in the outlet aqueous phase (up to 0.020 kg·m^{-3}) back up the good extraction efficiency in the mixing zone.

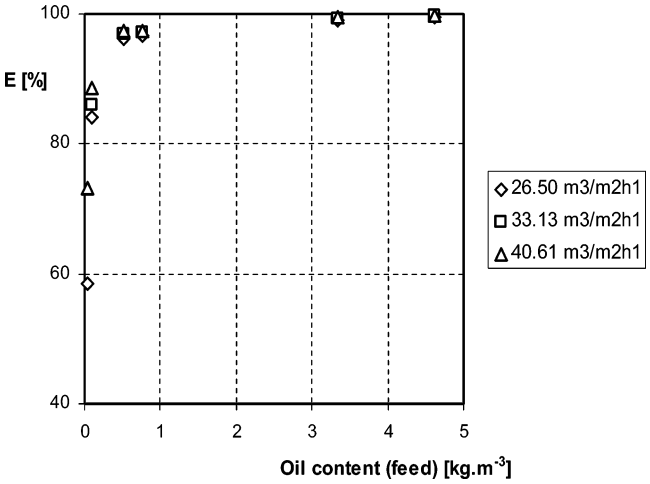

Figure 5. Influence of the initial oil content on the separation for various specific throughputs ($U_N = 0.14 \div 0.22$ m·s^{-1}; $O/A = 0.33$; $N = 750$ rpm).

It can be assumed that the coalescence probability will be proportional to the ratio $N_{oil}/N_{solvent}$, where N_{oil} is the number of oil droplets in the mixing zone (based on the mean oil droplet diameter and the oil concentration) and $N_{solvent}$ is the number of solvent drops (based on the mean drop diameter and the solvent concentration). The separation efficiency versus this ratio is plotted in Figure 7. As expected, the maximum separation for a given phase ratio is always obtained for the number of drops ratio higher than 0.05. Therefore, for a drops ratio up to 0.05, the separation calculated efficiency has to be modified as follows:

$$E_{final} = \left(\frac{N_{oil}}{N_{solvent}}\right)^{0.06} \times E \qquad (7)$$

The predicted separation efficiencies are compared to the experimental ones in Table 5. As it can be seen, the use of the new design method gives very good results with little scattering. The average deviation in most cases does not exceed ±6%.

4.3.2. Application to Industrial Wastewater (Formation of Water−Oil and a Hydrocarbon Mixture as Solvent). The

Table 6. Comparison between Experimental and Predicted Separation Efficiencies (Solvent Aguarras)

organic bed height (H_o) [m]	stirring speed [rpm]	initial oil content [kg·m^{-3}]	specific flow rate (Q) [m^3·m^{-2}·h^{-1}]	phase ratio (O/A)	exptl [%]	calcd [%]	deviation [%]	drop-size ratio $\bar{d}_{oil}/\bar{d}_{min}$
1	800	1.215−1.696	45.84	1/2	91.5	87.73	4.30	1.08
1	700	1.215−1.696	35.65	1/6	72.1	68.94	4.58	0.82
1	700	0.251−0.732	45.84	1/2	70.9	100.0	29.10	1.27
1	800	0.251−0.732	35.65	1/6	55.0	59.07	6.89	0.70
0.75	750	0.733−1.214	40.74	1/3	81.5	78.21	4.21	0.91
0.75	750	0.733−1.214	40.74	1/3	80.0	78.21	2.29	0.91
0.75	750	0.733−1.214	40.74	1/3	80.4	78.21	2.81	0.91
0.75	750	0.733−1.214	40.74	1/3	84.3	78.21	7.79	0.91
0.75	750	0.733−1.214	40.74	1/3	84.0	78.21	7.41	0.91
0.75	750	0.733−1.214	40.74	1/10	76.4	63.91	19.54	0.72
0.75	750	0.733−1.214	40.74	17/30	70.5	100.0	29.50	1.31
0.75	750	0.733−1.214	33.61	1/3	82.9	77.15	7.45	0.91
0.75	750	0.0500.−250	40.74	1/3	53.7	63.44	15.36	0.91
0.75	750	0.733−1.214	47.87	1/3	74.3	79.66	6.73	0.91
0.75	820	0.733−1.214	40.74	1/3	68.1	71.61	4.90	0.82
0.75	750	1.697−1.897	40.74	1/3	77.8	78.21	0.53	0.91
0.5	800	1.215−1.676	35.65	1/2	92.5	91.29	1.32	1.08
0.5	700	1.215−1.676	45.84	1/6	68.4	76.06	10.07	0.82
0.5	700	0.251−0.732	35.65	1/2	76.8	100.0	23.20	1.27
0.5	800	0.251−0.732	45.84	1/6	55.0	66.18	16.89	0.70

design method described above was applied to the new obtained results for a real industrial dispersion of crude oil/formation water coming from PETROBRÁS/E&P-RNCE (Ceará basin/Mandaú sub-basin and from the fields of Xeréu and Atum) and

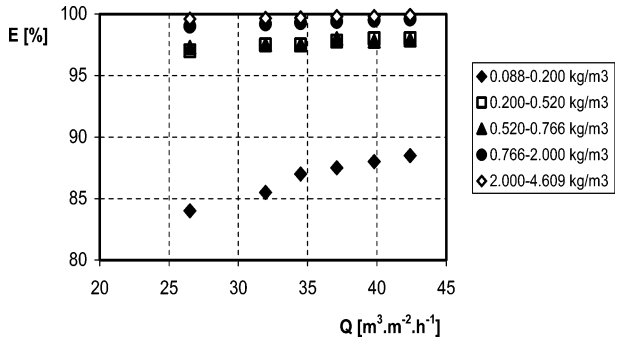

Figure 6. Influence of the total flow rate on separation ($U_N = 0.14 \div 0.22$ m·s^{-1}; $O/A = 0.33$; $N = 750$ rpm).

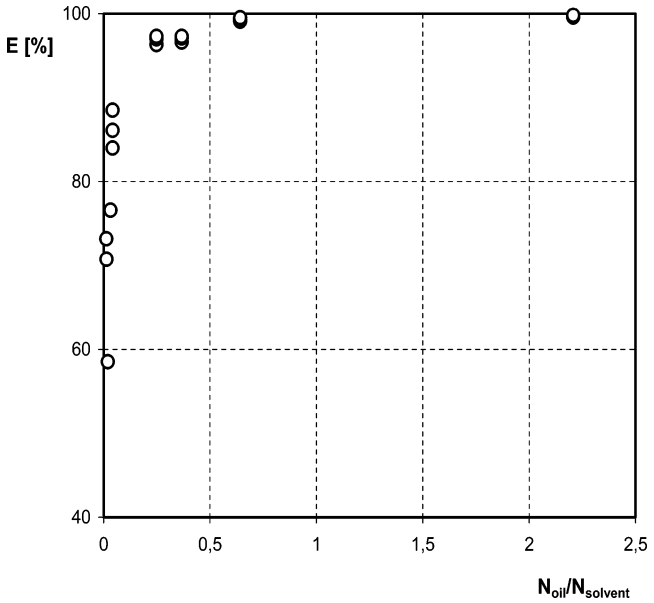

Figure 7. Influence of the coalescence probability on the separation efficiency ($U_N = 0.14 \div 0.28$ m·s^{-1}; $O/A = 0.20 \div 0.33$; $N = 750$ rpm; initial oil concentration 0.041 − 4.609 kg·m^{-3}; $Q = 26.50 \div 40.76$ m^3·m^{-2}·h^{-1}).

containing colloid clay particles.[8] The solvent was a hydrocarbon mixture (aguarras, PETROBRAS). The mean droplet diameter ($\bar{d}$) of the solvent dispersion was determined using the constants C_1 and C_2 given in Table 3. The difference between these proportionality constants (similar to those given in ref 16) and the above given values with system 1 is probably due to the role of the clay particles and their interaction with the Cl^- ions.

The predicted separation efficiencies are compared to the experimental ones in Table 6. As it can be seen, the use of the new design method can explain satisfactorily the low separation efficiencies, obtained in some experimental conditions. In all cases, when low efficiencies are observed, the mean droplet-size ratio ($\bar{d}/\bar{d}_{oil}$) was very different from the optimal one ($\bar{d}/\bar{d}_{oil} = 1 \pm 0.1$).

5. Conclusion

A new method is proposed to design the operating conditions in the mixing zone of a MSPI unit. It is based on the capacity of the settler to provide high separation efficiency while throughput increases. A number of correlations are identified that allow reasonable prediction of the $D_{3,2}$ values of carriers formed using a perforated plate, as well as the drop size distribution and the Sauter mean diameter ($d_{3,2}$) of the primary dispersion. They allow predicting the influence of the organic/aqueous phase ratio as well as the contact angle on these parameters. The method is applied to design operating conditions in MSPI devices used in two particular cases, a heavy metal extraction and a crude oil emulsion separation. A comparison with already obtained experimental results show that it is possible to determine the optimal operating conditions in the mixer-settler allowing for very good extraction efficiency coupled with good separation efficiency.

Notation

A = aqueous phase flow rate
b = baffle width
d = carried droplet diameter in eq 2
$\bar{d}$ = mean solvent drop diameter in the mixer
d_{imp} = impeller diameter
$D_{3,2}$ = Sauter mean carrier drop diameter
D_m = diameter of the mixing zone

d_{max} = maximum carried drop diameter in the mixer
$\bar{d}_{min}$ = minimal Sauter mean diameter (minimum mean carried droplet diameter to generate in the mixer)
d_N = nozzle diameter
$\bar{d}_{oil}$ = mean oil droplet diameter
D_s = diameter of the settling zone
E = overall separation efficiency
f = correction coefficient in eq 5
g = gravitational acceleration
H_m = height of the mixing zone
H_o = height of the organic bed in the settler
H_s = height of the settler
N_{oil} = number of oil droplets in the mixer
$N_{solvent}$ = number of solvent droplets in the mixer
O = organic phase flow rate
R_i = internal radius of the nozzle
Q = throughput
U_N = velocity in the nozzle of the scattering plate
Y = bottom clearance in the mixer

Greek Letters

ϕ = dispersed phase volume fraction
μ_{aq} = dynamic viscosity of the aqueous phase
μ_o = dynamic viscosity of the organic phase
ρ_{aq} = continuous phase density
ρ_o = organic phase density
$\Delta\rho$ = density difference
σ = interfacial tension
θ = contact angle

Literature Cited

(1) Treybal, R. *Liquid extraction*; McGraw-Hill: New York, 1963.
(2) Fitch, E. B. *Solid-Liquid Separations Equipment Scale-up*; Purchas, D.B., Ed. Academic Press: New York, 1986.
(3) Kyntch, G. J. *Trans. Faraday Soc.* **1951**, *48*, 166−176.
(4) Kyuchoukov, G.; Hadjiev, D. Bulgarian Patent 72358, 12.11, 1985.
(5) Hadjiev, D.; Kyuchoukov, G. A separator for liquid-liquid dispersions. *Chem. Eng. J.* **1989**, *41*, 113−116.
(6) Hadjiev, D.; Aurelle, Y. Phase inversion: A method for separation of fine liquid-liquid dispesions. *Chem. Eng. J.* **1995**, *58*, 45−51.
(7) Aurelle, Y.; Hadjiev, D.; Brounhonesque, M.; Damak, R.; Roques, H.; Kyuchoukov, G. New two phase liquid-liquid separators. *Technology Today, France* **1991**, *2*, 104.
(8) Paulo, J. B. A.; Fernandes, W. E., Jr.; Hadjiev, D. Solvent assisted method for the treatment of wastewaters contaminated with crude petroleum. Presented at 7th World Congress of Chemical Engineering, July 2005, Glasgow, Scotland.
(9) Paulo, J. B. A.; Hadjiev, D. Extraction separation in mixer-settler based on phase inversion, *Sep. Purif. Technol.* **2005**, *39*, 257−262.
(10) Hadjiev, D.; Limousy, L.; Sabiri, N. E. The design of separators based on phase inversion at low velocities in the nozzles. *Sep. Purif. Technol.* **2004**, *38*, 181−189.
(11) Horvath, M.; Steiner, L.; Hartland, S. *Can. J. Chem. Eng.* **1978**, *56*, 9−15.
(12) Kumar, A.; Hartland, S. *Can. J. Chem. Eng.* **1985**, *63*, 368−376.
(13) Skelland, A. H. P.; Johnson, K. R. *Can. J. Chem. Eng.* **1974**, *52*, 732−738.
(14) Dalingaros, W.; Kumar, A.; Hartland, S. Effect of physical properties and dispersed phase velocity on the size of drops produced at a multi-nozzle distributor. *Chem. Eng. Process.* **1986**, *20*, 95−102.
(15) Zhang, X. Dynamics of growth and breakup of viscous pendant drops into air. *J. Colloid Interface Sci.* **1999**, *212*, 107−122.
(16) Cull, S. G.; Lovick, J. W.; Lye, G. J.; Angeli, P. Scale-down studies on the hydrodynamics of two-liquid-phase biocatalytic reactors. *Bioprocess Biosyst. Eng.* **2002**, *25*, 143−153.
(17) Kumar, S.; Ganvir, V.; Satyanand, C.; Kumar, R.; Ghandi, K. S. Alternative mechanisms of drop breakup in stirred vessels. *Chem. Eng. Sci.* **1998**, *53*, 3269−3280.
(18) Chester, A. K. The modelling of coalescence processes in fluid-liquid dispersions: a review of current understanding. *Chem. Eng. Res. Des.* **1991**, *69*, 259−270.
(19) Kumar, S.; Kumar, R.; Ghandi, K. S. Alternative mechanisms of drop breakage in stirred vessels. *Chem. Eng. Sci.* **1991**, *46*, 2483−2489.
(20) Doulah, M. S. An effect of hold-up on drop sizes in liquid-liquid dispersions. *Ind. Eng. Chem. Fundam.* **1975**, *14*, 137−138.
(21) Pacek, A. W.; Man, C. C.; Nienow, A. W. On the Sauter mean diameter and size distributions in turbulent liquid-liquid dispersions in a stirred vessel. *Chem. Eng. Sci.* **1998**, *53*, 2005−2011.
(22) Boye, A. M.; Lo, M.-Y. A.; Shamlou, P. A. The effect of two-liquid phase rheology on drop breakage in mechanically stirred vessels. *Chem. Eng. Commun.* **1996**, *143*, 149−167.
(23) Paulo, J. B. A. *Mise au point d'un nouveau mélangeur − décanteur à inversion de phases. Application à l'extraction du cuivre*. Ph.D. Thesis, INP, Toulouse, France, 1996.
(24) Stone, H. A. Dynamics of drop deformation and break-up in viscous fluids. *Annu. Rev. Fluid Mech.* **1994**, *26*, 65−102.
(25) Yeung, A.; Moran, K.; Masliyah, J.; Czarnecki, J. Shear-induced coalescence of emulsified drops. *J. Colloid Interface Sci.* **2003**, *265*, 439−443.
(26) Lyu, S. P.; Bates, F. S.; Macosko, W. Modeling of coalescence in polymer blends. *AIChE J.* **2002**, *48*, 7−14.
(27) Paulo, J. B. A.; Chiavenato, M. C.; Hadjiev, D. Use of a new type of mixer-settler for the treatment of residual water contaminated with crude petroleum. Presented at Congrès Français du Génie des Procédés, Nancy, France, 2001.
(28) Desnoyer, C.; Masberant, O.; Gourdon, C. Experimental study of drop size distributions at high phase ratio in liquid-liquid dispersions. *Chem. Eng. Sci.* **2003**, *58*, 1353−1363.
(29) Zeichner, G. R.; Schowalter, W. R. Use of trajectory analysis to study stability of colloidal dispersions in flow fields. *AIChE J.* **1977**, *23*, 243.

Received for review February 3, 2005
Revised manuscript received March 6, 2006
Accepted March 28, 2006

IE050133Z